

CHAPTER XX-1

**THE SPY III IMMATURE TIBIA:
NEANDERTAL OR NEOLITHIC?****Libby COWGILL****Abstract**

While the diaphysis of an immature hominid tibia was discovered along with the original adult Spy Neandertal materials, it remains unclear whether the fragmentary tibia represents a juvenile Neandertal, or is derived from the larger sample of Neolithic remains from the site. Although it is not possible to resolve this issue conclusively without directly dating the specimen, this study aims to shed light on the taxonomic affinities of the immature tibial remains from Spy through an analysis of its mid-shaft cross-sectional properties and limb proportions. Adult Neandertals possess relatively shortened distal extremities that are consistent with cold adaptation. In addition, they display elevated levels of tibial robusticity (particularly relative to tibial length) when compared to Holocene populations. These two features may assist in differentiating the immature Spy tibia from Belgian Neolithic tibiae. The cross-sectional properties and estimated length of the immature tibial remains from Spy was compared to several large samples of immature Holocene humans from a broad selection of geographic locations, and to small samples of immature tibiae from both the Late Pleistocene tibiae and the Belgian Neolithic. The results of these analyses confirm that ecogeographic patterns in crural indices exist throughout ontogeny, and Late Pleistocene tibiae display elevated levels of diaphyseal robusticity at an early age. Based on the relatively modest cross-sectional properties of the Spy III tibia when compared to its length, it remains likely that this specimen does not represent an immature Neandertal, but is intrusive from overlying Neolithic layers.

INTRODUCTION

In addition to the diagnostically Neandertal material from the site of Spy, the fragmentary remains of an immature tibial diaphysis, designated Spy III, was also recovered. It is unclear, however, whether this element is of Late Pleistocene age, and is directly associated with the other Spy materials, or is intrusive and derived from the Neolithic deposits overlaying the Spy assemblage (see Rougier *et al.*, this volume: chapter XIX). Due to both its developmentally immature and fragmentary condition, it is impossible to assess the taxonomic affinities of this element based on external morphology alone; establishing provenience of the specimen is likely unattainable short of directly dating the specimen. Thus, it remains difficult to conclusively determine if the Spy III tibia is of Pleistocene or Holocene origin. However, despite the damaged condition of the Spy III tibia, a basic level of information may be gathered from this specimen, including length and age estimates. It may also be possible to evaluate at least one variable

characteristic of the Spy III tibia that could potentially shed light on its group affiliation: the biomechanical properties of its diaphysis.

The general pattern of adult variation in lower limb robusticity across the Late Pleistocene has been well documented. When cross-sectional properties of Neandertal tibia are scaled to biologically appropriate estimates of body mass, lower limb robusticity remains relatively constant during this time period (Trinkaus, 1997; Trinkaus & Ruff, 1999). However, due to ecogeographic patterning in body proportions, adult Neandertals possess relatively shortened distal limb segments and broad pelvic breadths (Trinkaus, 1981; Ruff, 1991, 1994; Holliday, 1997a, 1997b). When Neandertal tibial cross-sectional properties are standardised by length alone, Neandertal tibiae appear exceptionally robust relative to both Holocene comparative samples and Late Pleistocene contemporaries (Lovejoy & Trinkaus, 1980; Trinkaus & Ruff, 1999). While standardising cross-sectional properties by beam length alone is no longer con-

sidered the most appropriate standardisation method, it may prove useful as a heuristic device for achieving graphic separation between Neandertal tibiae and other groups.

Previous research on Holocene humans implies that relative levels of cross-sectional robusticity and ecogeographic body proportions are established early in ontogeny and maintained throughout growth (Cowgill, 2006, 2010; Cowgill & Hager, 2007). In addition, there is limited evidence that immature Neandertals were similar to adults in possessing shortened distal limb segments (Ruff *et al.*, 1994; Thompson & Nelson, 2005). This paper will attempt to apply the results of these prior analyses to the cross-sectional properties of the immature Spy III tibia in a relatively unconventional manner. In addition to presenting a brief discussion of the Spy III tibia morphology and a tentative estimation of its age, the cross-sectional properties of its diaphysis were evaluated relative to multiple comparative samples of immature tibiae, including a small group of Late Pleistocene individuals. With this in mind, the goals of this paper are twofold: first, to determine if it is possible to separate the tibial cross-sectional geometry of immature Neandertals from other groups due to the distal limb shortening and relatively robust tibia that are well-documented in adults; and second to evaluate the taxonomic affinities of the Spy III tibia in this context in order to determine whether it is best grouped with the Neandertal assemblage from Spy, or if it is likely to be intrusive material from the Belgian Neolithic.

MATERIALS

The Spy III tibia

The Spy III tibia is an immature diaphyseal fragment measuring 123.9 mm in length (Figure 1). The specimen is fractured proximally, with a transverse break extending across the anterior surface of the diaphysis, and a small (8 mm) piece of cortical bone projecting towards the proximal metaphysis on the posterior aspect of the broken surface. The broken edge of the specimen is just superior to the most proximal extent of a roughened and prominent soleal line on the posterior surface, which crosses the prox-



Figure 1. Anterior view of the Spy III tibia.
Photo courtesy of P. Semal, RBINS.

imal quarter of the fragment inferomedially. There is no trace of the nutrient foramen that is most commonly found on the proximal third of the posterior tibial surface (Scheuer & Black, 2005). Anteriorly, the fracture edge lies proximal to the most distal extent of the porous epiphyseal surface for the tibial tuberosity anteriorly. As the anterior crest proceeds distally, it curves medially and becomes less prominent and angular just superior to the distal fracture. The oblique distal fracture, which crosses the shaft superolaterally to inferomedially, is slightly proximal to the approximate midshaft of the tibia. The cross-section at midshaft is subtriangular with smoothly rounded borders. The specimen is designated as a left based on the lateral curvature of the anterior crest proximally, the medial curvature of the anterior crest distally, and the inferomedial orientation of the soleal line posteriorly.

Age-at-death estimation

No reliable indications of age-at-death are preserved for the Spy III material due to the fragmentary condition of the specimen. Despite associated difficulties, the best age indicator available is the estimated tibial length. Comparison of the Spy III tibial fragment with other immature tibial diaphyses of similar size suggests that approximately 62-65 % of the original length is preserved. This provides a complete intermetaphyseal length estimate of approximately 195 mm.

Multiple studies have recorded tibial length and age in modern children, but comparison of the Spy III tibial length with these standards may lead to substantial error due to differences in limb proportions and stature between the Spy III individual and modern American and European children. Tibial length standards based on radiographs from longitudinal studies 20th century Euro-American children result in an age estimate of 4-5 years of age (Anderson, 1964; Maresh, 1970; Gindhart, 1973). This age range, however, is likely to underestimate the true age of the Spy III individual, particularly if it is an immature Neandertal.

Given this, it may be more appropriate to estimate the age of the Spy III individual based on dentally-aged remains from a smaller-bodied

archaeological population. While this technique possesses the associated difficulty that age is not known but must be determined through crown and root formation, it allows the added benefit of being able to select populations likely to be more similar to the Spy III individual in stature. If, in addition to relatively small body size, the Spy III individual belonged to a cold-adapted Neandertal population with distal limb segment shortening, age estimates based on a modern Euro-American reference sample would further underestimate the actual age of the Spy III juvenile, due to their proportionally longer tibia. If this were the case, it is more appropriate to estimate age based on a smaller-bodied, cold-adapted sample. Accordingly, the age of the Spy III individual was also estimated using a regression formula developed from a sample of immature Inuits from the site of Point Hope, Alaska (ages 0-18 years, n = 41). Using a tibial intermetaphyseal length of 195 mm as the independent variable, a slightly older age estimate of 7.3 years is produced [$0.07058(\text{TIBIA LENGTH}) - 6.509 = \text{AGE}$; $r^2 = 0.897$; $p < 0.001$]. If, on the other hand, the Spy III tibia is derived from a Belgian Neolithic population, it would be more likely to possess temperate-climate body proportions, and is best compared to a European archaeological assemblage. A regression formula of age on tibial intermetaphyseal length using medieval European remains from the site of Mistihalj (ages 0-18, n = 42) yields an age of 6.4 years, still substantially older than the estimate derived from modern Euro-American standards [$0.05894(\text{TIBIA LENGTH}) - 5.336 = \text{AGE}$; $r^2 = 0.915$; $p < 0.001$]. Based on these considerations, a broad age range of 5.5 to 7.5 years of age is constructed for the Spy III individual.

Comparative materials

Comparative data for the Spy III juvenile was generated from the available sample of immature Late Pleistocene remains (Table 1). The developmental ages were determined using crown and root formation assessed through lateral mandibular radiographs, and following the developmental standards set by Smith (1991) and Liversidge & Molleson (2004). Otherwise, age was assessed using a population-appropriate regression formula of age against long bone length, in a manner similar to that detailed above for the Spy III tibia.

In addition, the Late Pleistocene data was compared to cross-sectional properties and crural indices from six Holocene samples of immature remains. For the analysis of crural indices, all individuals under the age of eighteen were included in order to evaluate the general pattern or change in body proportions during development ($n = 415$); individuals less than ten years of age were used in the analysis of cross-sectional geometry in order to

	Age Estimates	Aging Method
<i>Neandertals</i>		
Dederiyeh 1	1.25	Dental
Dederiyeh 2	1.67	Dental
Kebara 1 ²	0.45	Dental
Roc de Marsal 1 ¹	2.50	Dental
Shanidar 10 ²	1.71	Prediction
Le Moustier 1 ¹	14.55	Dental
Le Moustier 2	0.05	Dental
La Ferrassie 4b ²	0.15	Prediction
La Ferrassie 6	2.44	Prediction
Amud 7 ²	0.53	Dental
Undescribed Amud tibia ²	0.00	Prediction
<i>Modern Humans</i>		
Balla 1 ¹	1.50	Prediction
Lagar Velho 1	4.65	Dental
Maritza 1	6.96	Dental
Skhul 1	3.25	Dental
Skhul 8	8.50	Prediction
Yamashita-cho 1	6.00	Prediction
El Wad 10312	0.05	Prediction
Arene Candide 11	2.40	Dental
Arene Candide 5B	2.75	Dental
Arene Candide 8	5.47	Dental
Romanelli 3	0.93	Dental
La Madeleine 4	3.30	Dental
Cro-Magnon 5B	0.00	Prediction
Cro-Magnon 5E ²	0.02	Prediction
El Wad 10315 ¹	10.03	Dental
Sunghir 2 ¹	11.68	Dental
Arene Candide 15 ¹	15.90	Dental
Arene Candide 1 ¹	16.40	Dental
Dolní Věstonice 14 ¹	17.50	Dental
Taforalt	20 individuals	Primarily prediction

¹ Only used in analysis of crural indices

² Only used in analysis of cross-sectional geometry

Table 1. Late Pleistocene comparative samples, point estimates of ages, and aging methods.

be more directly comparable to the Spy III individual ($n = 300$). Four of the samples (Mistihalj, California Amerindian, Indian Knoll, and Point Hope) are from non-mechanised societies, with the later three being semi-sedentary foraging populations. In addition, a very small sample of Belgian Neolithic tibiae of similar size to the Spy III tibia were included in the analysis to provide an approximate estimation of the cross-sectional properties of this group ($n = 3$). Table 2 contains descriptions of each sample, sample sizes per population for the analysis of cross-sectional geometry, percentages of sample sizes dentally aged, and r-squared for the formula used to predict age in each sample.

METHODS

Reconstruction of cross-sectional geometry

The primary data for this analysis consists of the midshaft cross-sectional properties of immature tibiae. Two methods were used to reconstruct the immature tibial cross-sectional morphology. The cross-sections for all of the Holocene comparative sample and the majority of the Late Pleistocene sample (including Spy III) were reconstructed using the “latex cast method,” in which polysyllable molding putty (Cuttersil Putty Plus™) was used to transcribe the subperiosteal contours and biplanar radiography to generate parallax-corrected cortical thicknesses, from which the endosteal contours were interpolated (O’Neill & Ruff, 2004). All sections were projected enlarged and digitised, and the cross-sectional properties were computed from the resulting sections in a PC-DOS version of SLICE (Nagurka & Hayes, 1980; Eschman, 1992). External molding of several of the Late Pleistocene specimens was not possible, and the cross-sectional properties of these elements were reconstructed using the “ellipse model method,” which relies on anteroposterior and mediolateral radiographs alone (O’Neill & Ruff, 2004).

Comparisons involve regressions of total area (TA), cortical area (CA), percentage of cortical area, anteroposterior (I_x) versus mediolateral (I_y) second moments of area (I_x/I_y), maximum (I_{max}) versus minimum (I_{min}) second moments of area (I_{max}/I_{min}), and the polar second moment of

<i>Sample</i>	<i>Sample Description</i>	<i>Location</i>	<i>N</i>	<i>Percentage Dentally Aged</i>	<i>r² for Age Regression</i>
Dart Collection	20th century, ethnically mixed Southern Africans	University of Witwatersrand, Johannesburg, South Africa	43	90.7 %	0.890
Mistihalj	Medieval Eastern Europeans from Serbia	Harvard Peabody Museum	36	100.0 %	0.877
Indian Knoll	North American Archaic period Native Americans from Kentucky	University of Kentucky at Lexington	67	76.1 %	0.922
Point Hope	Pre- and proto-historic Alaskan Inuits	American Museum of Natural History	27	85.2 %	0.888
California Amerindian	Mixed sample of Native American remains from multiple sites in Northern California	Phoebe Hearst Museum, University of California, Berkeley	56	56.0 %	0.928
Kulubnarti*	Medieval Christians from Sudanese Nubia	University of Colorado, Boulder	71	98.6 %	0.896
<i>Total</i>			267	81.6 %	

* Only used in crural index analysis

Table 2. Sample description, sizes, and location for comparative sample under the age of ten years. Percentage of each sample dentally aged, and the r^2 for the age-prediction regression based on femur or tibia length also shown.

area (J) on age. Cross-sectional areas are generally proportional to strength during axial loading. Second moments of area are calculated to express the bending strength of the bone in different planes: I_x and I_y quantify the bending strength of the bone in the anteroposterior and mediolateral planes, respectively, while I_{max} and I_{min} measure the maximum and minimum bending strength of the diaphysis. Polar second moments of area provide a general measure of the element's overall bending and torsional strength and are calculated from the sum of I_{max} and I_{min} (Ruff & Hayes, 1983). In analyses of cross-sectional properties seeking to draw conclusions about activity levels or biomechanical strength, cross-sectional properties of weight-bearing elements should be standardised by a mechanically relevant measurement of body size (Ruff *et al.*, 1993). However, since this analysis is attempting to group the Spy III tibia with either Holocene or Late Pleistocene populations based on variation in cross-sectional properties relative to tibial length, powers of biomechanical intermetaphyseal length are employed. Accordingly, cross-sectional areas were standardised by tibia length³ and polar second moments of area standardised by tibia length^{5.33} (Ruff *et al.*, 1993).

Statistical analysis

For both the analysis of crural indices and cross-sectional properties, statistical comparisons were undertaken using the comparative sample as a general baseline against which the Spy III tibia and other Late Pleistocene fossil specimens were evaluated. In order to investigate patterns of relative tibia length during growth, crural indices were regressed on age. Standardised residuals from this regression were used to determine if immature individuals exhibit variation similar to adults in ecogeographic body proportions, and if immature Neandertals are likely to possess relatively shortened distal limb segments. In addition, the samples were divided into several biologically relevant age categories (0-1.9 years, 2-4.9 years, 5-7.9 years, 8-10.9 years, 11-13.9 years, 14-17.9 years) in order to examine how crural indices vary with age in greater detail.

Given the non-linear trajectory of human robusticity growth curves (Ruff, 2003), all cross-sectional data was smoothed relative to age using a robust locally weighted regression technique, LOESS (Cleveland, 1979, 1994), and the patterns of variation were visually assessed relative

to the LOESS line. If the relationship between cross-sectional properties and age in specific age categories was sufficiently linear, a linear regression was fit to the data in order to generate residuals reflecting the relationship of the Spy III individual to other Holocene and Pleistocene individuals within a similar age range.

RESULTS

Body proportions

The results of this analysis support the interpretation that crural indices vary during development. Crural indices are highest in infancy, reach a low by approximately ten years of age, and rise again during adolescence (Table 3).

The best fit line for this relationship is a quadratic equation [$p < 0.001$; $CRURAL = 0.8450 - 0.0050(AGE) + 0.0003(AGE^2)$], although neither a linear nor a quadratic equation explains much of the variation crural index ($r^2 = 0.002$ and $r^2 = 0.064$,

<i>Age Category</i>	<i>Sample Size</i>	<i>Mean</i>	<i>Confidence Interval</i>
Age Category 1 (0 to 1.9 years)	129	0.842	0.837-0.847
Age Category 2 (2 to 4.9 years)	66	0.831	0.824-0.837
Age Category 3 (5 to 7.9 years)	74	0.830	0.823-0.837
Age Category 4 (8 to 10.9 years)	67	0.822	0.815-0.829
Age Category 5 (11 to 13.9 years)	47	0.831	0.821-0.840
Age Category 6 (14 to 17.9 years)	66	0.835	0.828-0.842

Table 3. Age category means, samples sizes, and confidence intervals for crural index.

respectively; Figure 2). In addition, there is populational variation in crural indices throughout growth. Standardised residuals from the quadratic

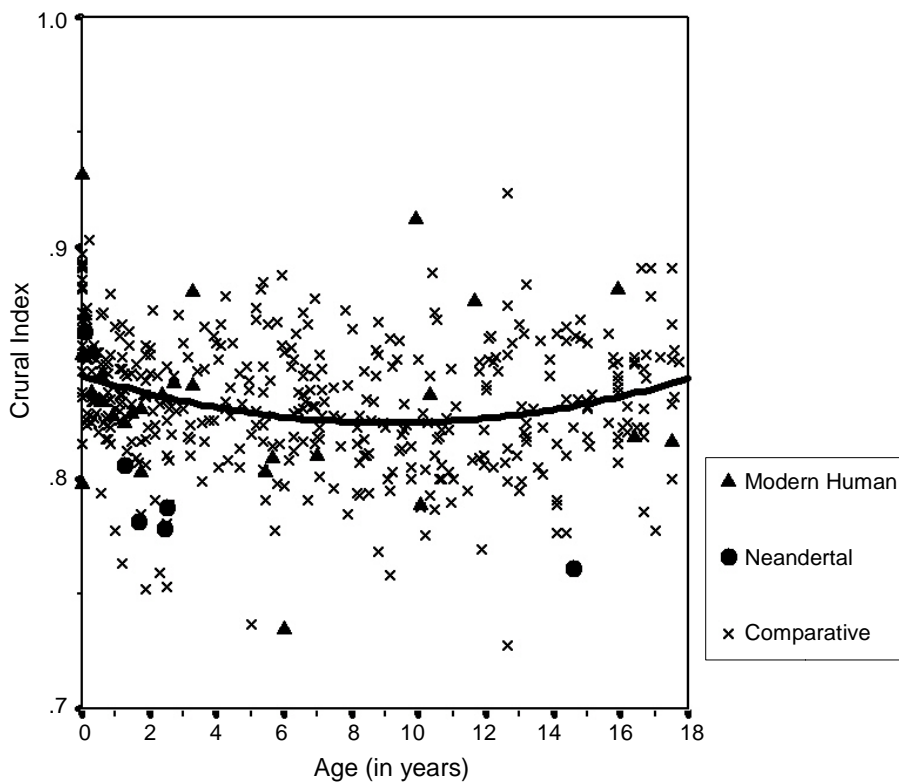


Figure 2. Relationship between crural index and age among recent humans, Neandertals, and Pleistocene modern humans, illustrated with a quadratic equation.

regression of crural index on age illustrate that populations generally follow the trends that would be predicted based on ecogeographic adaptations to climate (Table 4). The African, Native American, and early modern human samples display positive residuals, while the European, Arctic, and Neandertal juveniles all exhibit negative residuals. Based on these analyses, it is probably appropriate to assume that the distal limb segment shortening that is characteristic of Neandertal adults also typifies Neandertal body proportions prior to maturity. Thus, if the Spy III tibia is that of a Neandertal, it is best to age it based on the archaeological population displaying low crural indices (Point Hope) and to expect that it will possess diaphyseal properties that are relatively high when compared to its length.

Cross-sectional geometric properties

The cross-sectional geometric properties of the Spy III tibia are shown in Table 5. In general, the patterns of developmental variation for standardised total area, cortical area, and polar second moments of area are similar to those

<i>Sample</i>	<i>Standardised Residual Mean</i>
California Amerindian	0.0588
Dart	0.2070
Indian Knoll	0.1258
Mistihalj	-0.4556
Point Hope	-1.1275
Kulubnarti	0.5652
Neandertal	-1.4379
Pleistocene EMH	0.0420

Table 4. Standardised residual mean by sample from the regression of crural index on age.

described previously among smaller samples of recent humans (Ruff *et al.*, 1994; Trinkaus & Ruff, 1996; Cowgill *et al.*, 2007). When standardised by powers of length, total area, cortical area, and polar second moment of area all display high values in infancy, followed by a rapid decline, and then stabilisation through later childhood (Figure 3). As predicted, with the exception of cortical area for Shanidar 10 and Dederiyeh 2, the cross-sectional properties of immature Neandertals generally fall between the middle and upper range of modern human variation. If the sample is restricted to individuals between the ages of five and ten years of age, a linear regression can be fit to the data, from which standardised residuals can be generated. While there are unfortunately no comparative Neandertal data within this age range, the resultant residuals from the regressions for total area, cortical area, and polar second moments of area illustrate that the cross-sectional properties of the Spy III individual lay between those of the Neolithic comparative material, who fall well below the regression line, and the Late Pleistocene early modern humans, who plot far above it (Table 6).

The bivariate plot of tibial midshaft percentage of cortical area on age reveals a pattern that has been documented in other samples (Van Gerven *et al.*, 1985); variation in tibial percentage of cortical area is characterised by a steep decline during the first two years postnatal, followed by a shallow rise which is continued into adulthood (Figure 4). The Spy III tibia displays a low, but unremarkable, percentage of cortical area, and plots with the similarly aged Neolithic tibia. As illustrated by the plot of maximum versus minimum second moments of area on age (Figure 5), all tibiae become relatively less round with age. The ratio of maximum to minimum second moments of area for the Spy III tibia is quite low for its age. In this parameter, the Neandertals are too young for direct comparison

	TA^1	CA^1	I_x^2	I_y^2	I_{max}^2	I_{min}^2	J^2	Θ
Spy III	169.6	124.5	2325.9	2052.9	2397.1	1981.7	4378.8	65.6

¹ Cross-sectional moments of area in mm²

² Second moments of area in mm⁴

Table 5. Midshaft cross-sectional parameters for the Spy III tibia.

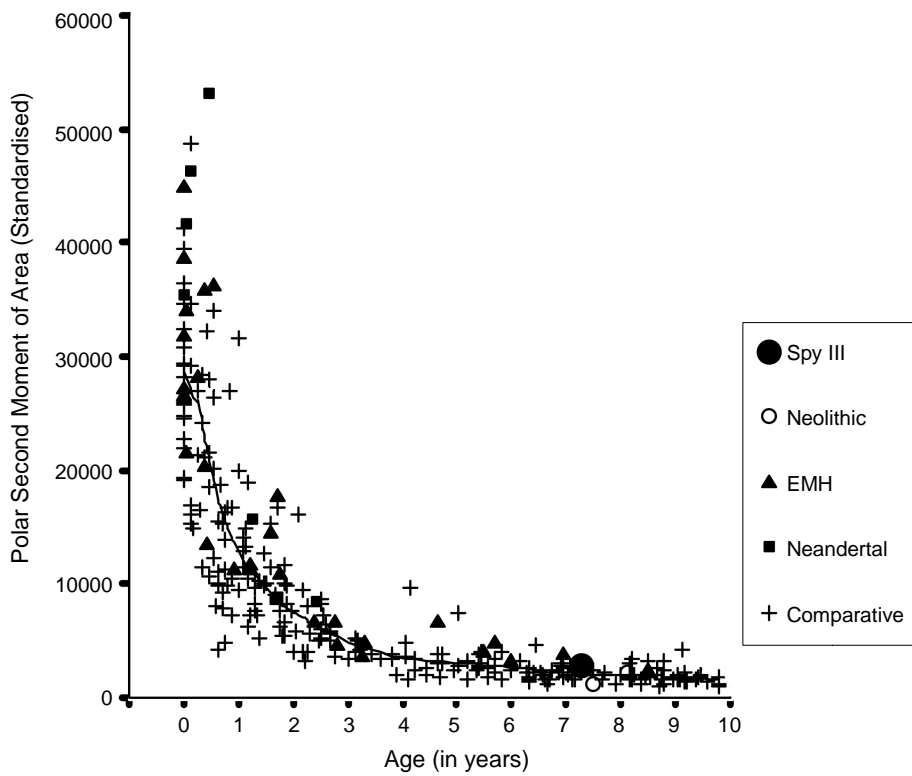


Figure 3. Bivariate plot with LOESS regression line of tibial midshaft standardised polar second moment of area versus age for Spy III, Neandertals, early modern humans, and Holocene human comparative samples.

to the Spy III tibia and the Late Pleistocene modern humans show considerable variation, but it is clear that the Spy III tibia is unlike the three Neolithic specimens, who fall higher in the range of variation.

DISCUSSION

While several tentative conclusions can be drawn from the above analyses, the various limitations of this study must first be acknowledged.

		<i>Total Area</i>	<i>Cortical Area</i>	<i>J</i>	<i>Max/Min</i>
Pleistocene Modern Humans	Mean	1.1978372	1.285838	1.2307618	-0.1188447
	N	5	5	5	4
	STD	0.52882925	0.89372644	0.72846202	0.8470775
	Minimum	0.42986	-0.12168	0.51278	-0.96727
	Maximum	1.82009	2.34916	2.22095	0.90511
Neolithic Comparative	Mean	-0.8440745	-0.9160078	-0.7363351	0.7611731
	N	3	3	3	3
	STD	0.77030468	0.97451405	0.79914105	0.16825681
	Minimum	-1.36332	-1.6327	-1.27572	0.6246
	Maximum	0.04097	0.19363	0.18176	0.94913
<i>Spy III</i>		<i>0.6871926</i>	<i>0.4293221</i>	<i>0.4473043</i>	<i>-1.724422</i>

Table 6. Standardised residuals means from the regression of total area (TA), cortical area (CA), polar second moment of area (J), and max/min second moments of area on age for Spy III, Late Pleistocene modern humans, and the Neolithic comparative material.

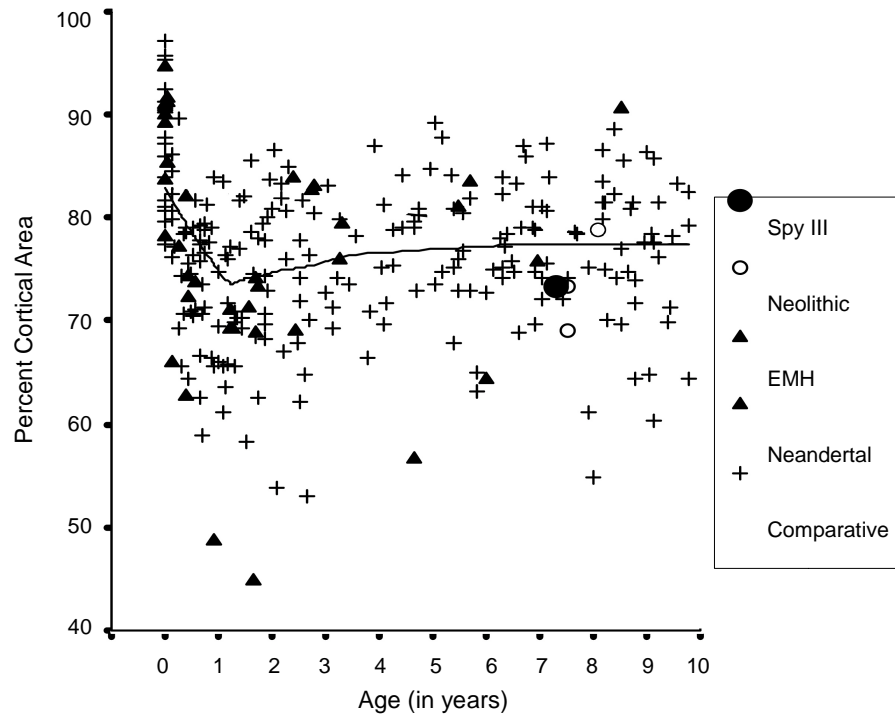


Figure 4. Bivariate plot with LOESS regression line of tibial midshaft percentage of cortical area on age for Spy III, Neandertals, early modern humans, and Holocene human comparative samples.

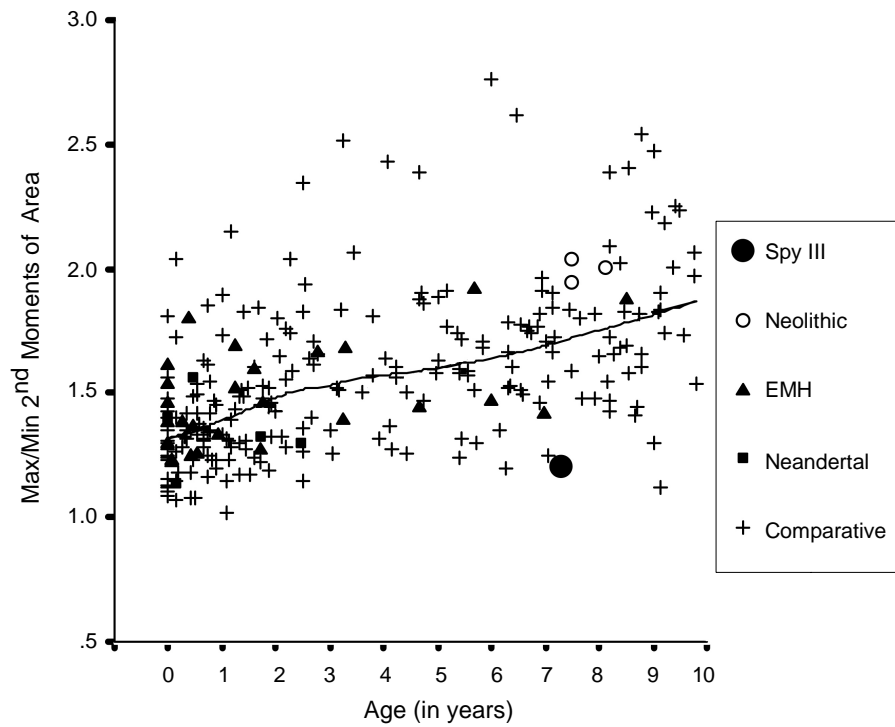


Figure 5. Bivariate plot with LOESS regression line of tibial midshaft maximum/minimum second moments of area (I_{\max}/I_{\min}) versus age for Spy III, Neandertals, early modern humans, and Holocene human comparative samples.

In order to evaluate the cross-sectional properties of the Spy III tibia relative to an appropriate developmental cohort, it was first necessary to undertake several levels of estimation.

First, since length was estimated, it is possible that errors in length could have affected the results of the above analyses, particularly because the cross-sectional properties were standardised by powers of length. Closer inspection of the data, however, reveals that in order for the errors to impact the interpretation of these analyses, the error in the estimated length would have to be quite large. For example, in order for the Spy III tibia to possess a standardised cortical area as large as the mean for the Late Pleistocene modern humans, the Spy III cortical area would have to be standardised by a tibial length almost 15 millimetres less than the current estimate. Given the length of the original fragment and the landmarks preserved, estimation errors of this magnitude seem unlikely.

Second, while age was estimated based on length, it does not appear that even large errors in the determination of the developmental age of the Spy III tibia would greatly affect the results of the above analyses. Because of the general shape of the growth curve, shifting the developmental age of Spy III from the upper range of the estimated ages (7.3 years, based on prediction from Inuit regression formulae) to the lower end of the estimated range (5.5 years) does nothing to alter the *relative* position of the Spy III tibia in comparison to the Neolithic and Late Pleistocene individuals.

Third, no Neandertal tibiae were available in the immediate developmental cohort of the Spy III tibia, and comparisons had to be made between the Spy individual and Late Pleistocene early modern humans.

Even with these considerations fully in mind, it is nonetheless difficult to support the argument that the Spy III tibial remains represent an immature Neandertal, based on the analyses presented here. The analysis of the residuals derived from the regression of total area, cortical area, and polar second moment of area on age reveal that even between the ages of five and

ten, Late Pleistocene individuals are displaying the high level of lower limb robusticity relative to tibial length that they possess as adults. In addition, since the immature Late Pleistocene early modern humans likely possess the temperate and tropical climate body proportions of the adults in their respective populations, standardising their cross-sectional properties by uncorrected powers of length could actually *reduce* their apparent robusticity. While there are no immature Neandertal tibiae available in the immediate age group of the Spy III tibia, previous analyses of adults indicate that their respective level of lower limb robusticity is comparable to that of the early modern humans (Trinkaus, 1997; Trinkaus & Ruff, 1999).

The analysis of subadult body proportions undertaken above implies that standardising the cross-sectional properties of immature Neandertals by powers of tibial length would only *increase* their apparent robusticity relative to both Late Pleistocene modern humans and the Holocene comparative sample. Thus, if the Spy III tibia represents an immature Neandertal, it is developmentally exceptional in possessing a tibia significantly less robust than its contemporaries.

CONCLUSIONS

It has been well documented within the palaeoanthropological literature that adult Neandertals possess tibiae that are relatively robust in relationship to their length. This research has attempted to evaluate the taxonomic affinities of the immature tibial diaphysis from Spy based on its apparent midshaft robusticity relative to tibial length. The results of this research support the idea that, like the adults in their respective populations, immature Neandertals also displayed cold-adapted shortening of their distal limb segments and displayed the elevated levels of lower limb robusticity characteristic of Late Pleistocene individuals in general. While one analysis cannot conclusively rule out the possibility that the Spy III individual is a Neandertal, its relatively modest cross-sectional properties when compared to similarly aged Late Pleistocene individuals suggests that it may be intrusive from Neolithic layers.

BIBLIOGRAPHY

- ANDERSON M., BLAIS MESSNER M. & GREEN W. T., 1964. Distribution of lengths of the normal femur and tibia in children from one to eighteen years of age. *Journal of Bone and Joint Surgery*, **46**: 1197-1202.
- CLEVELAND W. S., 1979. Robust locally weighted regression and smoothing scatterplots. *American Journal of the Statistical Association*, **74**: 289-336.
- CLEVELAND W. S., 1994. *The Elements of Graphing Data*. New Jersey, Murray Hill.
- COWGILL L. W., 2006. Postcranial growth and development of immature skeletons from Point Hope, Alaska. *American Journal of Physical Anthropology*, **129** (S42): 78 (abstract).
- COWGILL L. W., 2010. The ontogeny of Holocene and Late Pleistocene human postcranial strength. *American Journal of Physical Anthropology*, **141** (1): 16-37.
- COWGILL L. W. & HAGER L. D., 2007. Variation in the development of postcranial robusticity: an example from Çatalhöyük, Turkey. *International Journal of Osteoarchaeology*, **17**: 235-252.
- COWGILL L. W., TRINKAUS E. & ZEDER M. A., 2007. Shanidar 10: A Middle Paleolithic Immature Distal Lower Limb from Shanidar Cave, Iraqi Kurdistan. *Journal of Human Evolution*, **53** (2): 213-223.
- ESCHMAN P. N., 1992. *SLCOMM Version 1.6*. Albuquerque, NM, Eschman Archaeological Services.
- GINDHART P. S., 1973. Growth standards to the tibia and radius in children aged one month through eighteen years. *American Journal of Physical Anthropology*, **39** (1): 41-48.
- HOLLIDAY T. W., 1997a. Body proportions in Late Pleistocene Europe and modern human origins. *Journal of Human Evolution*, **32** (5): 423-447.
- HOLLIDAY T. W., 1997b. Postcranial evidence of cold adaptation in European Neandertals. *American Journal of Physical Anthropology*, **104** (2): 245-258.
- LIVERSIDGE H. M. & MOLLESON T., 2004. Variation in crown and root formation and eruption of human deciduous teeth. *American Journal of Physical Anthropology*, **123** (2): 172-180.
- LOVEJOY C. O. & TRINKAUS E., 1980. Strength and robusticity of the Neandertal tibia. *American Journal of Physical Anthropology*, **53** (2): 465-470.
- MARESH M. M., 1970. Measurements from roentgenograms. In: R. W. McCAMMON (ed.), *Human Growth and Development*. Springfield, Charles C. Thomas: 157-200.
- NAGURKA M. L. & HAYES W. C., 1980. An interactive graphics package for calculating cross sectional properties of complex shapes. *Journal of Biomechanics*, **13**: 59-64.
- O'NEILL M. C. & RUFF C. B., 2004. Estimating human long bone cross-sectional geometric properties: a comparison of noninvasive methods. *Journal of Human Evolution*, **47** (4): 221-235.
- RUFF C. B., 1991. Climate, body size and body shape in hominid evolution. *Journal of Human Evolution*, **21** (2): 81-105.
- RUFF C. B., 1994. Morphological adaptation to climate in modern and fossil hominids. *Yearbook of Physical Anthropology*, **37**: 65-107.
- RUFF C. B., 2003. Ontogenetic adaptation to bipedalism: age changes in femoral to humeral length and strength proportions in humans, with a comparison to baboons. *Journal of Human Evolution*, **45** (4): 317-349.
- RUFF C. B. & HAYES W. C., 1983. Cross-sectional geometry of Pecos Pueblo femora and tibiae—a biomechanical investigation: I. Method and general patterns of variation. *American Journal of Physical Anthropology*, **60** (3): 359-381.
- RUFF C. B., TRINKAUS E., WALKER A. & LARSEN C. S., 1993. Postcranial robusticity in *Homo*. I: Temporal trends and mechanical interpretation. *American Journal of Physical Anthropology*, **91** (1): 21-53.
- RUFF C. B., WALKER A. & TRINKAUS E., 1994. Postcranial robusticity in *Homo*. III: Ontogeny. *American Journal of Physical Anthropology*, **93** (1): 35-54.
- SCHEUER L. & BLACK S., 2000. *Developmental Juvenile Osteology*. London, Elsevier Academic Press.
- SMITH B. H., 1991. Standards of human tooth formation and dental age assessment. In: M. A. KELLEY & C. S. LARSEN (ed.), *Advances in Dental Anthropology*. New York, Wiley-Liss: 143-168.

- THOMPSON J. L. & NELSON A. J., 2005. The postcranial skeleton of Le Moustier 1. *In*: H. ULLRICH (ed.), *The Neandertal Adolescent Le Moustier 1: New aspects, new results*. Berlin, Staatliche Museen zu Berlin, Preußischer Kulturbesitz: 265-281.
- TRINKAUS E., 1981. Neandertal limb proportions and cold adaptation. *In*: C. B. STRINGER (ed.), *Aspects of Human Evolution*. London, Taylor & Francis: 187-224.
- TRINKAUS E., 1997. Appendicular robusticity and the paleobiology of modern human emergence. *Proceedings of the National Academy of Sciences USA*, **94**: 13367-13373.
- TRINKAUS E. & RUFF C. B., 1996. Early modern human remains from eastern Asia: the Yamashita-cho 1 immature postcrania. *Journal of Human Evolution*, **30** (4): 299-314.
- TRINKAUS E. & RUFF C. B., 1999. Diaphyseal cross-sectional geometry of near eastern Middle Paleolithic humans: The tibia. *Journal of Archaeological Sciences*, **26** (10): 1289-1300.
- VAN GERVEN D. P., HUMMERT J. R. & BURR D. B., 1985. Cortical bone maintenance and geometry of the tibia in Prehistoric children from Nubia's Batn el Hajar. *American Journal of Physical Anthropology*, **66** (3): 275-280.

AUTHOR'S AFFILIATION

Libby COWGILL
Department of Anthropology
University of Missouri, Columbia
213C Swallow Hall
Columbia, MO 65211-1440
USA
cowgilll@missouri.edu